Ultrasonics 65 (2016) 194–199

Contents lists available at ScienceDirect

Ultrasonics

journal homepage: www.elsevier.com/locate/ultras

Semi-analytical modeling of acoustic beam divergence in homogeneous anisotropic half-spaces

Naoyuki Kono [a,*], Sohichi Hirose [b]

[a] Center for Technology Innovation – Energy, Research & Development Group, Hitachi, Ltd., 7-2-1 Omika-cho, Hitachi-shi, Ibaraki 319-1221, Japan
[b] Department of Mechanical and Environmental Informatics, Tokyo Institute of Technology, 2-12-1 O-okayama, Meguro-ku, Tokyo 152-8552, Japan

ARTICLE INFO

Article history:
Received 28 April 2015
Received in revised form 13 September 2015
Accepted 2 October 2015
Available online 13 October 2015

Keywords:
Anisotropy
Attenuation
Divergence
Scattering
Austenitic steel

ABSTRACT

Beam divergences of acoustical fields in semi-infinite homogeneous anisotropic media are calculated based on a semi-analytical model. The model for a plane source in a semi-infinite homogeneous anisotropic medium is proposed as an extended model for a point source in an infinite medium. Beam divergences propagating along crystallographic axes $\langle 100 \rangle$, $\langle 110 \rangle$, and $\langle 111 \rangle$ in a cubic crystal, a single crystalline Ni-based alloy, are measured and compared to calculation results for verifying the model. The contribution of beam divergence attenuation to the total attenuation for propagating in anisotropic polycrystalline materials is quantitatively evaluated in isolation from scattering attenuation effects.

1. Introduction

Austenitic steels showing acoustical anisotropy are widely used in the main components of power plants as heat-resistant and/or corrosion-resistant alloys. Ultrasonic propagation behavior in weld metals and cast steels made of austenitic steels, e.g. stainless steels 316 and Ni-based alloys 600, is more complicated than that of isotropic media, such as base metal made of ferrite steels, and may cause low signal-to-noise ratio and beam skewing in beam propagation [1]. Especially, solidification structures like welds indicate strong acoustical anisotropy.

For improvement of non-destructive evaluation (NDE) of austenitic steel welds, optimization of ultrasonic testing conditions is essential by understanding propagation and scattering behaviors. In austenitic welds, these behaviors are very complex because of polycrystalline structure composed of many grains with varying size and orientation. Research works have been reported for understanding propagation behavior by modeling, e.g. ray-tracing [2,3], multi-Gaussian [4], and EFIT [5]. Attenuation of ultrasonic beam is arisen from both scattering at grain boundaries and beam divergence. Therefore, quantitative evaluation of scattering behavior is difficult because of mixing extracting scattering and divergence effects. In this paper, we propose a quantitative modeling of beam divergence for indirect evaluation of scattering effect.

The solidified structure of the austenitic steels is polycrystalline and composed of cubic crystalline grains. The crystal growth orientation of the austenitic steels is aligned along the crystal axis $\langle 100 \rangle$, and crystal orientations along the other axes normal to the $\langle 100 \rangle$ axis are distributed randomly. The solidified structure is locally regarded as a unidirectional solidification; therefore, the solidified structure is macroscopically treated as a transversely isotropic crystal system.

Ultrasonic propagation behavior in austenitic steel welds has been reported since the late 1970s. The angular dependence of velocity and attenuation are reported in both the theoretical and experimental aspects [6–10]. Anisotropy of the austenitic welds is treated as a model based on transversely isotropic crystal systems, and the model is consistent with experiments with respect to the angular dependence of the velocity.

However, with regard to the angular dependence of attenuation, it has been reported that the measured attenuation results are inconsistent with the prediction of scattering theories for polycrystalline materials: the measured attenuation shows minimal value for an approximately 45-degree angle between the beam propagation direction and crystal growth direction [11]; the theories predict an attenuation increase with an increasing angle between the beam propagation and the crystal growth angles.

* Corresponding author. Tel.: +81 294 52 9256; fax: +81 294 52 8803.
E-mail address: naoyuki.kono.jm@hitachi.com (N. Kono).

http://dx.doi.org/10.1016/j.ultras.2015.10.004
0041-624X/

Several comparisons between measured attenuation and theoretical attenuation have been reported. Scattering attenuation effects have been obtained from the measured amplitude through phase correction for received waves by Seldis [12–14]. For a theoretical approach, semi-analytical modeling for anisotropic material has been reported by Spies [15]. Beam skewing and beam divergence effects are calculated numerically for specific crystalline axes. However, the beam divergence attenuation dependency on crystalline axes has been evaluated qualitatively.

A model for a plane source in a semi-infinite anisotropic medium is proposed in this study. The model is extended from a model for a point source in an infinite anisotropic medium, which was originally proposed by Buchwald [16]. Beam divergence attenuation is evaluated quantitatively by means of the extended model. The extended model is verified by comparison with experiments for a single crystalline material.

Additionally, the contribution of beam divergence attenuation to the total attenuation for propagating in austenitic welds is quantitatively estimated based on the extended model applied to a transversely isotropic medium. The angular dependence of beam divergence attenuation is discussed separately from scattering attenuation.

2. Theory

The equations of motion for elastic waves are expressed by Eq. (1):

$$c_{ijkl}u_{k,lj} + f_i = \rho \ddot{u}_i, \tag{1}$$

where c_{ijkl} is the stiffness tensor, u_i is the displacement vector, ρ is the density, f_i is the body force per unit volume, $u_{k,lj} = \partial^2 u_k/\partial x_l \partial x_j$, and $\ddot{u}_i = \partial^2 u_i/\partial t^2$.

First, assume that the body force is a time-harmonic point source acting at the origin in the mth direction in an infinite domain, as shown in Fig. 1(a). Thus, the ith component of the unit body force is expressed as $f_i = f_i^{(m)} = \delta_{im}\delta(\mathbf{x})e^{-i\omega t}$, using the angular frequency ω.

Let $U_{im}(\mathbf{x}, t)$ be the ith component of the displacement at point $\mathbf{x}$ due to the point force acting in the mth direction at the origin. The displacement has the same time vibration as the point force after some elapsed time; therefore, $U_{im}(\mathbf{x}, t)$ can be expressed by $U_{im}(\mathbf{x}, t) = \overline{U}_{im}(\mathbf{x})e^{-i\omega t}$. The function $\overline{U}_{im}(\mathbf{x})$ satisfies the following equations:

$$c_{ijkl}\overline{U}_{km,lj}(\mathbf{x}) + \delta_{im}\delta(\mathbf{x}) = -\rho\omega^2\overline{U}_{im}(\mathbf{x}). \tag{2}$$

According to Buchwald [16], $\overline{U}_{im}(\mathbf{x})$ is obtained by applying the Fourier transform and its inverse in space to Eq. (2), and then $\overline{U}_{im}(\mathbf{x})$ can be approximately expressed as:

$$U_{im}(\mathbf{x}, t) = \sum_{s_3^p} \frac{1}{2\pi|k_1^p k_2^p|^{1/2}} \cdot \frac{C_{im}}{\partial S/\partial s_3} \cdot \frac{\exp\left[i\omega(s_3^p x_3) - t\right]}{x_3} \times \exp\left(\frac{i\pi}{4}\sigma^p\right), \tag{3}$$

where k_1 and k_2 are the principal curvatures of slowness and s_i is a component of the slowness vector $\mathbf{s}$. S is the determinant of the matrix $S_{ik} = C_{ijkl}s_j s_l - \rho\delta_{ik}$, C_{im} is the adjoint matrix of the matrix $\mathbf{S}$, and σ^p is defined by $\sigma^p = \operatorname{sgn} k_1^p + \operatorname{sgn} k_2^p$. In Eq. (3), an observation point is located at the point $P(0, 0, x_3)$ far enough from the point source, and s_j^p is a slowness vector component of the normal on the slowness surface, which is parallel to $\overrightarrow{OP}$.

When the body force per unit volume is given by $f_i = F_0(\mathbf{x})e_i e^{-i\omega t}$ and is distributed in domain D, the displacement vector u_i is expressed in the convolution integral of U_{ik} and F_i:

$$u_k(\mathbf{x}, t) = \int_D U_{ik}(\mathbf{x} - \mathbf{y}, t)F_0(\mathbf{y})e_i dV_y, \tag{4}$$

where e_i is the unit vector component.

As shown in Fig. 2, the surface traction on S_T is considered to be equivalent to the body force action in the thin domain with surface S_T and thickness ε. Since $F_0(\mathbf{x})\mathbf{e}\,dV = P_0(\mathbf{x})\mathbf{e}\,dS$ and $P_0(\mathbf{x}) = F_0(\mathbf{x})\varepsilon$, Eq. (3) can be written in a surface integral form:

$$u_k = \int_{S_T} U_{ik}(\mathbf{x}-\mathbf{y}, t)P_0(\mathbf{y})e_i dS_y = \int_{S_T} \sum_{s_3^p} \frac{1}{2\pi|k_1^p k_2^p|^{1/2}} \cdot \frac{P_0(\mathbf{y})C_{ik}e_i}{\partial S/\partial s_3} \cdot \frac{\exp\left[i\omega s_3^p(x_3 - y_3) - t\right]}{x_3^p} \exp\left(\frac{i\pi}{4}\sigma^p\right) dS_y, \tag{5}$$

Note that in Eq. (5), the positive x_3-direction is always kept in the direction $(\mathbf{x} - \mathbf{y})$ by rotating the axes depending on source position $\mathbf{y}$, and x_3^p is the distance between point O and P.

In Eq. (5), the integrand consists of the first part with the same dimension as the reciprocal of velocity, the second part depending on the source term $P_0 C_{ik} e_i$, and the third exponential part that is inversely proportional to the distance: $x_3^p = \overline{OP}$.

A simplified expression of the second part can be obtained by algebraic calculations [17–19]. The adjoint matrix of the matrix $\mathbf{S}$ is proportional to the products of polarization vectors $\mathbf{p}$ (eigenvectors of the matrix $\mathbf{S}$):

$$C_{ik} = tr(\mathbf{S})p_i p_k. \tag{6}$$

The denominator of the second part of the integrand in Eq. (5) is expressed as Eq. (7):

$$\partial S/\partial s_j = C_{ik}\partial S_{ik}/\partial s_j = \mathrm{tr}(\mathbf{S})c_{ijkl}s_l p_i p_k = \mathrm{tr}(\mathbf{S})\rho V_j^{\mathrm{group}} \tag{7}$$

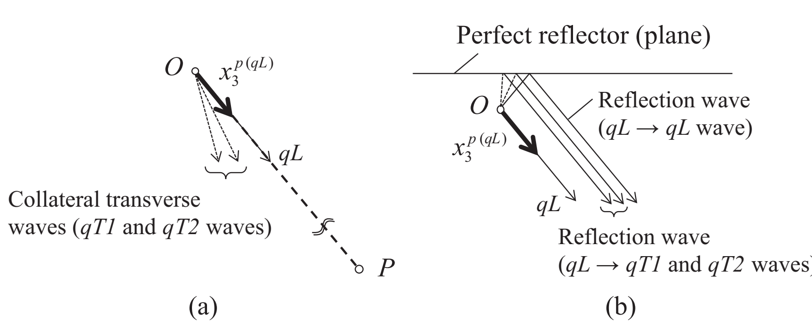

Fig. 1. Geometric conditions for infinite and half-space solids. (a) Infinite solid, and (b) half-space solid.